Liquefaction Controlling Components and Their Effect on Carbon-Free Mold Powders

NATHALIE GRUBER

In the continuous casting of ultra-low carbon steels, recarburization from the mold powder negatively affects steel quality. Therefore, to develop mold powders without free carbon, different carbides or nitrides have been proposed and evaluated in laboratory and field studies. Among these, SiC and Si_3N_4 were selected for the present study. Additionally, thermodynamic calculations were performed to quantitatively describe their effect on the melting behavior of the mold powder. To verify the results under high heating rates, mixtures of raw material components were placed in a steel crucible with a lid, inserted into a furnace preheated to different temperatures, and investigated mineralogically. The results agreed with those of the thermodynamic calculations. Moreover, the results suggested that Si_3N_4 and SiC were suitable raw material components and alternatives to carbon in the mold powder. They prevented solid–solid reactions between raw material components to form new phases and were still found at the temperature of 1200 °C. Consequently, the CaO/SiO_2 ratio was higher before oxidation and affected the liquid-phase formation. The addition of antioxidants reduced the liquefaction-controlling effect of SiC. Additionally, the study shows that the sample preparation impacts the phase formation: granules facilitate phase formation due to a higher contact of reactants, further they show earlier melting close to their surface as sodium content is increased there by the spray drying procedure.

I. INTRODUCTION

MOLD powder is an essential component in the continuous casting of steel; it is added to the top of the liquid steel in the mold to protect the steel from re-oxidation and minimize the heat loss. The temperature determines the existence of three horizontal layers: first, the original mold powder remains in contact with the environment; second, a sintered layer is formed with new solid and liquid phases; third, a liquid slag layer is present in contact with the steel.[1] To control the melting behavior of mold powders, different carbon carriers, such as carbon black or graphite, are used; these carriers reduce the contact between solid raw material particles to delay solid–solid reactions at lower temperatures and between liquid droplets to prevent the formation of a continuous liquid phase, which is known as the skeleton effect.[2–5] Depending on the oxygen supply, carbon is burned off with increasing temperature. If it is not totally removed during melting, it accumulates on top of the liquid slag layer, increasing its content. For example, the carbon content increases from 3.5 wt pct in the delivered state to 21 wt pct,[6] which has been validated by laboratory investigations.[7] The oscillation of the casting mold causes the liquid steel to come in contact with the carbon-enriched layer. Additionally, the turbulence of steel flow from the submerged entry nozzle (SEN) and unsteady state casting results in the recarburization of steel and changes its properties, combined with reduced product quality, specifically for ultralow carbon steels. To prevent this process, increased slag layer thicknesses impede the contact between the carbon and steel. Additionally, various methods have been developed to decrease the carbon content of the carbon-enriched layer, including the addition of an oxidizing agent, such as MnO_2, using the quick-burning-type carbons and activated carbons, or addition of Fe_2O_3, which acts as a catalyst for carbon oxidation at high temperatures and low oxygen activity.[8–11] Furthermore, developing a mold powder, wherein carbon is replaced as the liquefaction-controlling additive is necessary. Therefore, ceramic materials with low wettability by slags have been investigated as substitutes for carbon.[12–15] Initially, nitrides were used to control the melting behavior of the mold powders. Although various nitrides (BN,

NATHALIE GRUBER is with the Montanuniversitaet Leoben – Chair of Ceramics, Peter Tunner Straße 5, 8700 Leoben, Austria. Contact e-mail: nathalie.gruber@unileoben.ac.at

Table I. Mixture Compositions of Samples MP1–MP8 in Wt Pct

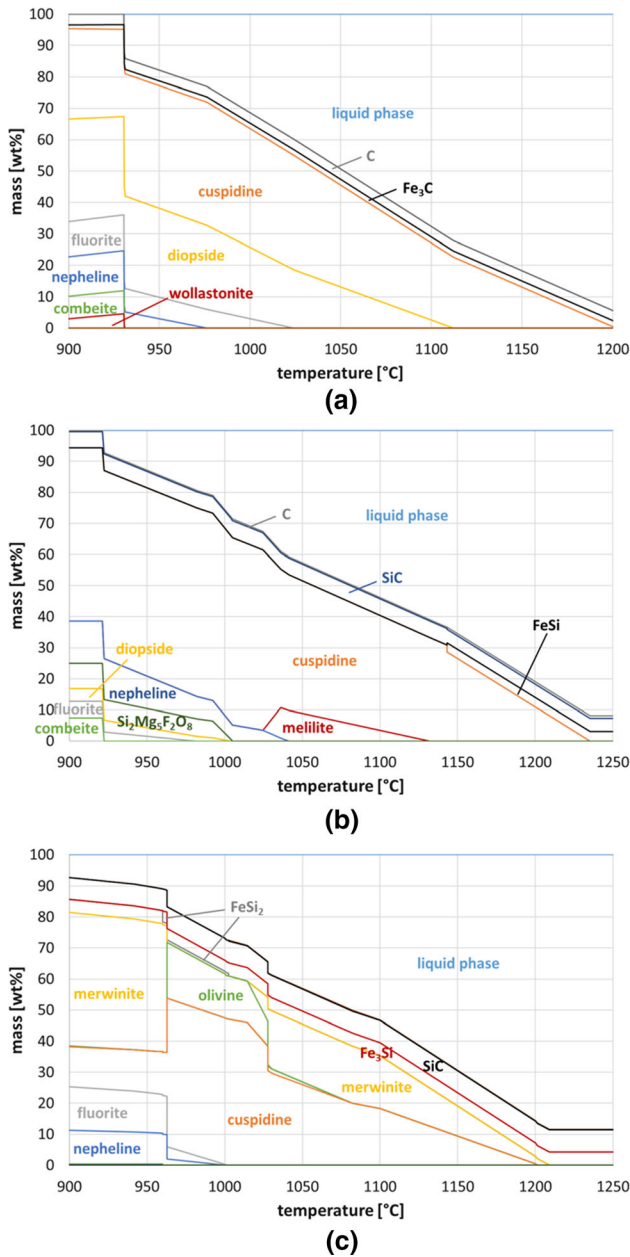|	MP 1	MP 2	MP 3	MP 4	MP 5	MP 6	MP 7	MP 8
	No Melting-Controlling Additive	With Carbon	With SiC	SiC, Antiox. Si	SiC, Antiox. Al	SiC, Antiox. Si and Al	Antiox. Al	With Si$_3$N$_4$
Quartz	6.8	6.9	6.3			0.3		
Feldspar	4.3	4.9	3.8			3.6		
Calcite	2.1	3.3	17.8	7.6		12.0		3.0
Fly ash	13.3	11.1	13.0	7.4				16.0
Glass					4.9	8.1	22.7	
Magnesite	9.4	9.1	8.1	9.5	10.9	9.3	9.9	9.3
Fluorite	19.5	18.7	18.7	19.5	20.4	19.2	20.3	19.8
Carbon		4.4						
Wollastonite	38.1	35.7	20.0	34.0	45.5	28.6	39.9	37.1
Soda	5.3	4.9	5.1	6.1	6.3	4.0	2.5	6.2
Corundum				2.4		0.7		0.5
Blast Furnace Slag				2.7	0.5	2.8		
SiC			6.0	6.5	6.8	6.4		
Hematite	1.3	1.2	1.2	1.7	2.4	2.3	2.4	1.2
Si met.				2.60		1.3		
Al met.					2.3	1.3	2.3	
Si$_3$N$_4$								6.9

Fig. 1—Mineral compositions as a function of temperature for (a) MP 0 and MP2, (b) MP 3, and (c) MP 4.

Si_3N_4, MnN, CrN, FeN, AlN, TiN, or ZrN) were tested.[9,12,13] BN was suggested as the best option owing to its similar crystalline structure to carbon and its high contact angle to slags. Furthermore, laboratory investigations revealed that mold powders containing BN have reduced sintering tendency and low gas evolution tendency compared with samples containing carbon black as a melting-controlling additive. As the melting rate decreases with the increasing particle size of all raw material components, the necessary amount of BN in the mold powder is defined by the ratio of the base material and BN particle sizes. The fusion rate of the original mold powder was compared with those of BN-containing mixtures, and similar results were obtained for samples containing 2 to 10 wt pct of BN. When BN is oxidized during heating, B_2O_3 acts as a fluxing agent, reducing the temperature of liquid-phase formation in the mold powder. Therefore, adding Al or CaSi as an antioxidant causes the liquefaction of the mold powder to occur at higher temperatures. Experiments have shown that when BN is added as the melting-controlling additive, suitable viscosity values for the continuous casting are obtained solely for mold slags with a CaO/SiO_2 ratio of 0.9. The newly developed BN-containing mold powder was tested during the continuous casting of a selected steel grade. Investigations of the bloom surface showed that nitride was also introduced into the liquid steel, which is as detrimental as carbon in terms of product quality. Therefore, its content must be reduced, but a reliable reduction is only possible if carbon is not completely removed.[9,12,13]

Another alternative to carbon as a melting-controlling additive is Si_3N_4. Its oxidation leads to the formation of SiO_2, which becomes part of the liquid slag later, and its low sintering tendency is considered advantageous. Laboratory investigations indicate that an average particle size of 5 μm and a specific surface of 2.5 to 3.5 m^2 g^{-1} are necessary to achieve the desired properties. Although industrial trials resulted in suitable melting rates of these mold powders, the steel underwent nitriding.[14–17]

Macho et al.[18] attempted to develop color-coded mold powders for each associated steel grade to prevent confusion during service, which required the elimination of carbon from the mold powder composition. When examined with a heating microscope, these color-coded products showed approximately the same softening, melting, and flowing points as the carbon-containing ones; however, their melting rate increased. The authors claimed that it does not negatively affect the casting process as long as a layer of the original mold powder was present on the surface.

SiC was also proposed as a melt-controlling additive to replace free carbon in mold powders. Samples containing 5 to 6 pct SiC showed a similar melting rate to conventional mold powders containing 2 to 2.5 wt pct of carbon. Further investigations of layers formed during the experiment revealed differences in the three layers compared with those of carbon-containing samples. Although the powder layer of the SiC-containing specimen was very thin, the sintered layer significantly increased. The oxidation of SiC decreased the mold powder basicity, promoting the formation of the liquid phase. Therefore, the total free carbon content was not replaced by SiC. However, investigations in contact with liquid steel revealed a considerably increased recarburization tendency when the free carbon content exceeded 1 wt pct.[16,19–22]

The aforementioned studies described primarily used phenomenological laboratory methods to investigate the melting behavior of standard mold powders compared with samples where the other melt-controlling additives replaced carbon. However, their effect during melting has not been comprehensively discussed. Therefore, based on the results summarized above, SiC with and

	$l_{1000\,°C}$ [wt pct]	T_s [°C]	T_l [°C]	$C_{residual}$ [g]	$SiC_{residual}$ [g]	SiC_{added} [g]	Si_3N_4 [g]	$Si_{3}N_{4\,added}$ [g]
MP 0	28.3	931	1202	3.24				
MP 1	26.7	923	1190					
MP 2	28.3	931	1202	3.24				
MP 3	24.2	922	1235	0.75	4.29	5.99		
MP 4	26.8	847	1209		7.07	7.07		
MP 5	18.8	852	1225		6.98	6.98		
MP 6	24.3	852	1210		7.04	7.04		
MP 7	27.5	927	1216					
MP 8	25.1	922	1235				4.94	6.87

$l_{1000°C}$ amount of liquid phase at 1000 °C, T_s solidus temperature, T_l liquidus temperature, $_{residual}$ quantity of the respective melt-controlling additive at 1550 °C, $_{added}$ initial quantity of the respective melt-controlling additive in the sample.

without antioxidants and Si_3N_4 were selected as carbon replacements and investigated in the laboratory experiments.

II. EXPERIMENTAL

A mold powder used for the continuous casting of ultralow carbon steels (MP 0) was selected. In the first step, 25 wt pct SiO_2 content in the mold powder was replaced by SiC or Si_3N_4 without changing the overall composition of the slag present after liquefaction and oxidation of the raw material components. Antioxidants are widely used in refractory materials to prevent oxidation of carbon.[23–25] Consequently, Al and Si were added to SiC to investigate their effect compared with the sample containing only SiC. Additionally, a specimen without melt-controlling components was analyzed to quantify the impact of each additive. Depending on the additive combination, each sample composition was standardized and adjusted to 100 pct for phase calculation using the thermochemical software FactSage. The dependence of phase composition on temperature was calculated without adding oxygen up to 1550 °C, representing the temperature of the liquid steel in the mold. The quantity of the phases present in dependence on temperature were depicted in diagrams. Furthermore, the amount of liquid phase at 1000 °C was calculated as an indicator for the melting tendency of the respective sample. To verify the accuracy of the obtained results, the samples were investigated after the heat treatment in a laboratory furnace. Based on the chemical composition of the raw materials, mixtures with the lowest discrepancy in chemical composition to the as-received mold powder after oxidation were defined. The following raw materials commonly used for the production of mold powders were selected: quartz, feldspar, calcite, fly ash, glass, magnesite, fluorite, carbon, wollastonite, soda, corundum, blast furnace slag, and hematite. SiC, Si, Al, and Si_3N_4 are used to control melting of the specimen. The raw material components used for each mold powder mixture MP1–MP8 are listed in Table I. 200 g of each sample were mixed and for each temperature treatment approximately 20 g of this mixture inserted into a steel

crucible ($30 \times 30 \times 40$ mm³), which was covered with a steel lid. To ensure high heating rates of the samples, the crucibles were introduced into a chamber furnace preheated to a defined temperature between 900 and 1200 °C under normal atmospheric conditions. Carbon, SiC, Al, Si, or Si_3N_4 will partly oxidize in the crucible atmosphere. Their oxidation is incomplete at least at lower temperatures; oxygen transport is hindered by the lid. This aims to simulate oxygen support under service conditions by diffusion. After a dwell time of 10 minutes, the crucibles were quenched to room temperature in air. Polished sections of the samples were prepared (embedded in resin and polished) and mineralogically investigated using reflected light microscopy and scanning electron microscopy coupled with energy-dispersive X-ray spectroscopy to quantify the chemical compositions of the phases in dependence on temperature. The chemical compositions are then assigned to mineral phases of this composition. For simplification, the results of the energy-dispersive X-ray spectroscopy are not depicted in the figures, but the respective mineral phases are indicated. Subsequently, the samples were ground for the X-ray diffraction analysis. The obtained results from laboratory investigations were then compared to the results from thermochemical calculations.

III. RESULTS AND DISCUSSION

A. Thermodynamic Calculations

Depending on the composition of the mold powders MP 0 to 8, the mineralogical compositions were calculated at the equilibrium. The quantity of different phases in dependence on temperature for selected samples are depicted in diagrams (Figure 1). Although most solid phases formed with increasing temperature were present in all samples, there were noticeable differences, particularly in their stability range. Except for samples wherein iron oxide is reduced to form solid iron or iron silicide of varying Fe/Si ratios, cuspidine [$Ca_4(Si_2O_7)(F,OH)_2$] is the last solid phase originating from the reactions of the raw materials during heating. At lower temperatures up to approximately 1000 °C, all samples contained nepheline ($Na_3KAl_4Si_4O_{16}$), and combeite
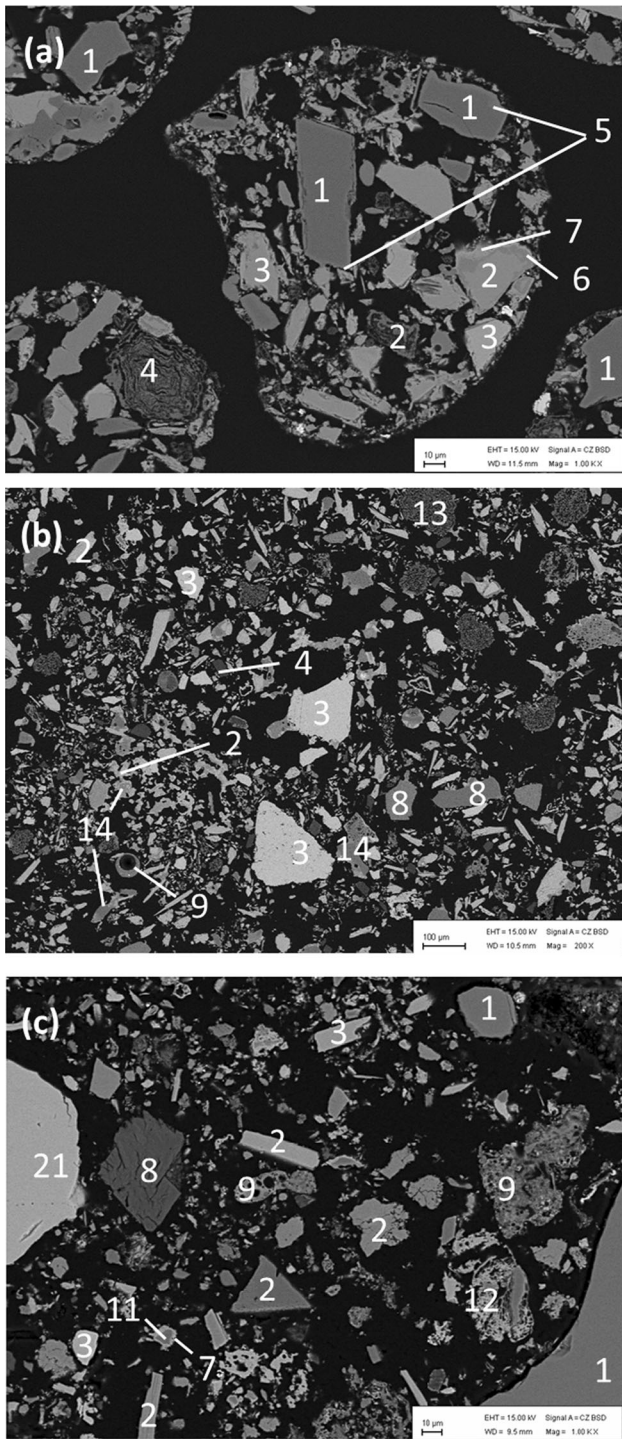
Fig. 2—Backscattered electron image of (*a*) MP 0, (*b*) MP 3, and (*c*) MP 4 after temperature treatment at 900 °C for 10 minutes. (1) albite, (2) wollastonite, (3) fluorite, (4) dissociated magnesite, (5) flourpectolite, (6) sodium calcium silicate, (7) cuspidine, (8) SiC, (9) fly ash, (10) quartz, (11) slag, (12) calcite, (13) corundum, and (14) liquid phase.

$(Na_2Ca_2Si_3O_9)$ was present in MP 0–3 and MP 8, along with fluorite (CaF_2). In MP 3 [Figure 1(b)] and MP 8, a magnesium fluoride silicate $(Mg_5F_2Si_2O_8)$ was also formed.

The cuspidine amount increased when SiO_2 was replaced with SiC or Si_3N_4 (MP 3 and MP 8) because of the reduced availability of SiO_2 caused by the incomplete oxidation of SiC. Consequently, silicate phases with higher SiO_2 contents, such as diopside $(CaMgSi_2O_6)$, which can be found in MP 0 and MP 1 [Figure 1(a)], are not stable in these samples [Figure 1(b)]. Similar behavior can also be observed for samples containing SiC and antioxidants, where cuspidine coexists with merwinite $[Ca_3Mg(SiO_4)_2]$, olivine $[(Mg, Fe)_2SiO_4]$, or melilite $[(Ca, Na)_2(Al, Mg, Fe^{2+})(Al, Si)SiO_7]$ instead of clinopyroxene. In contrast, the cuspidine amount did not increase significantly [Figure 1(c)]. However, with increasing temperature, SiC oxidation decreased the CaO/SiO_2 ratio. Because of the increased CaO/SiO_2 ratio at lower temperatures, the liquid-phase formation is delayed, which is not the case for carbon-containing mold powders.

To evaluate the melting tendency of samples, the amount of liquid phase at 1000 °C ($l_{1000°C}$) was calculated in addition to determining the solidus (T_s) and liquidus temperatures (T_l) (see Table II). The results revealed that the addition of melt-controlling additives (solely SiC and Si_3N_4) did not affect the temperature of the first liquid phase. Furthermore, the amount of liquid phase at 1000 °C was not influenced significantly, except in the case of MP 5, which showed the lowest amount of liquid phase. In contrast, the highest liquidus temperature was achieved for MP 3 after replacing carbon with SiC. This effect is reduced with the addition of antioxidants. The results indicate that the addition of antioxidants to SiC supports the formation of the first liquid phase because the temperature decreases by approximately 80 °C. Although the liquid was present at lower temperatures, its amount at 1000 °C was slightly higher than that of MP 3 and lower than that of MP 1 and 2.

For the FactSage calculations with no oxygen added, the samples did not totally liquefy up to 1550 °C as long as the melt-controlling additives (carbon, SiC, or Si_3N_4) were not completely oxidized. The phases still stable at 1550 °C according to the calculated results (their quantity is > 0 wt pct at 1550 °C) are marked by the subscript "residual" in Table II. For comparison their initial quantity is also given in the table and labeled with "added."

B. Mineralogical Investigations

After the temperature treatment at 900 °C, the standard mold powder (MP 0) showed the beginning of cuspidine formation accompanied by the formation of sodium calcium silicate separating the wollastonite $(CaSiO_3)$ center from the cuspidine rim, resulting in the diffusion of Na_2O into wollastonite [Figure 2(a)]. A thin reaction layer of flourpectolite $(NaCa_2Si_3O_8F)$ can be found at the borders of the albite particles. Magnesite is partly decarburized, and the fluorine diffuses from fluorite (CaF_2) into the residual magnesite. MP 1 and MP 2 showed similar appearances. In both the samples, diopside $(CaMgSi_2O_6)$ is formed additionally. In contrast, for the sample containing SiC (MP 3), no reactions of the raw material components were detected
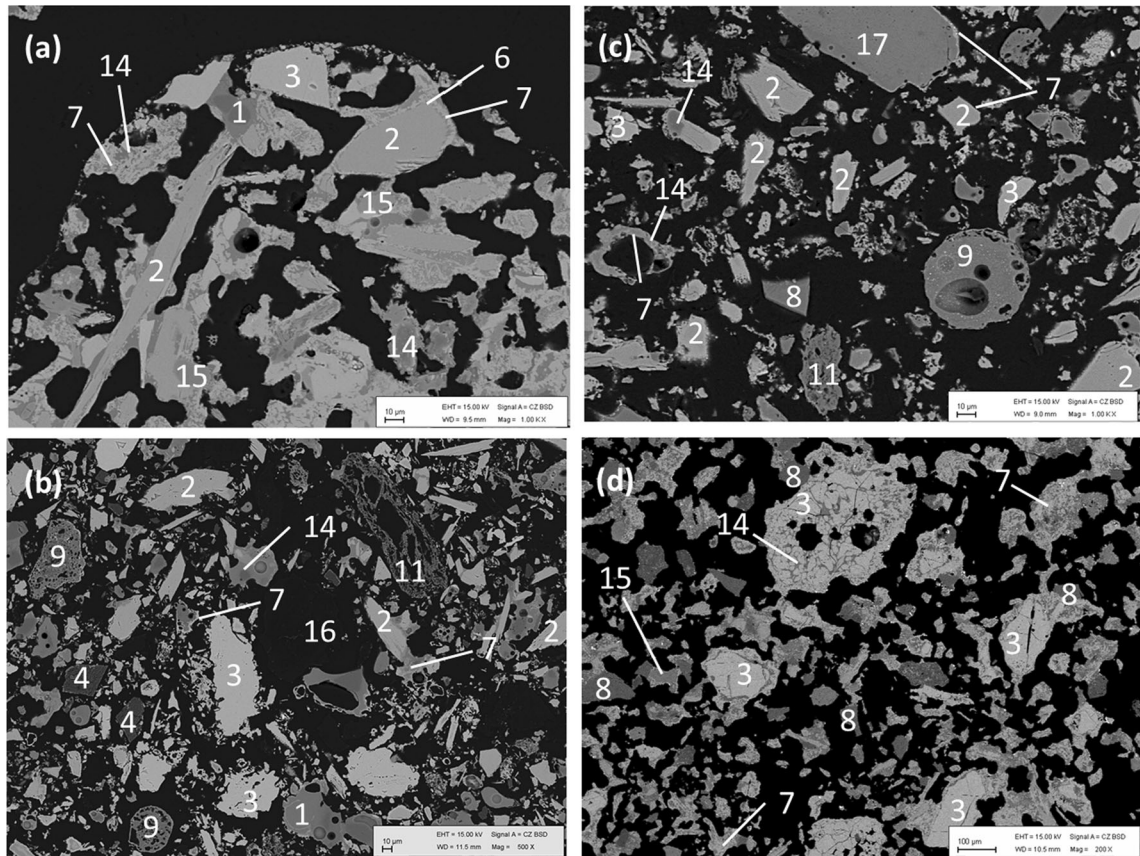
Fig. 3—Backscattered electron image of (*a*) MP 0, (*b*) MP 2, (*c*) MP 3, and (*d*) MP 5 after temperature treatment at 1000 °C for 10 minutes. (1) albite, (2) wollastonite, (3) fluorite, (4) dissociated magnesite, (6) sodium calcium silicate, (7) cuspidine, (8) SiC, (9) fly ash, (11) slag, (14) liquid phase, (15) diopside, (16) graphite, and (17) feldspar.

[Figure 2(b)]. This behavior changes by adding any antioxidant to SiC [Figure 2(c)]. Aluminum and silicon are already oxidized, and their oxides support the formation of the first liquid phase. Therefore, for the samples MP 4 to 6, even sintering of the fines can be detected at this temperature. The formation of cuspidine and sodium calcium silicates and dissociation of carbonates also occurred. Aluminum gets oxidized when added to the mixture, and F and Si diffuse into the aluminum oxide with the increasing temperature. Replacing carbon with silicon nitride resulted in small amounts of liquid phase owing to the diffusion of Na_2O into small glassy particles, further reducing their melting temperature. In addition, the diffusion of F into dissociated magnesite was observed.

Mineralogical investigations of the samples after annealing at 1000 °C revealed considerable differences in their melting behaviors. The as-delivered mold powder (MP 0) only showed residues of raw material particles in small amounts [Figure 3(a)], particularly wollastonite, fluorite, and albite ($NaAlSi_3O_8$). Cuspidine is present at the edges of large wollastonite particles. Wollastonite in the center and cuspidine at the edges are separated by sodium calcium silicate. Cuspidine originating from the reaction of the small raw material particles is mainly in contact with the liquid phase. When no liquefaction-controlling additives are used

(MP 1) at this temperature, new phases also form at the particle edges: Cuspidine is present at the surface of the former wollastonite, magnesite is decarburized, and F diffuses into the residues. The content of Na_2O at the particle surfaces of silica-containing raw materials further increases. However, no formation of the liquid phase occurs. Similar behavior can be noted for MP 2 [Figure 3(b)]. In contrast, MP 3 [Figure 3(c)] reveals hardly any reaction products, even at this temperature. Cuspidine is formed marginally, originating from the reactions of the fines. Owing to the presence of SiC, solid–solid reactions are inhibited, and formation of the new phases is shifted to higher temperatures. As observed at 900 °C, adding Al and Si as antioxidants to SiC forms silicon and aluminum oxide, which supports the formation of a liquid phase and new solid phase. For MP 4, a high sintering tendency is observed, and residuals only of rather large singular raw material particles are detected. SiC is partly oxidized, and SiO_2 starts to react with its surrounding components. This can be observed from the rounded shape of the original particles. However, the same effect was not observed after adding Al because the amount of liquid phase and cuspidine is relatively lower in MP 5 [Figure 3(d)], and the quantity of the raw material residuals is higher. Similar behavior was observed for MP 6. The sample with only Al addition (MP 7) reveals the highest
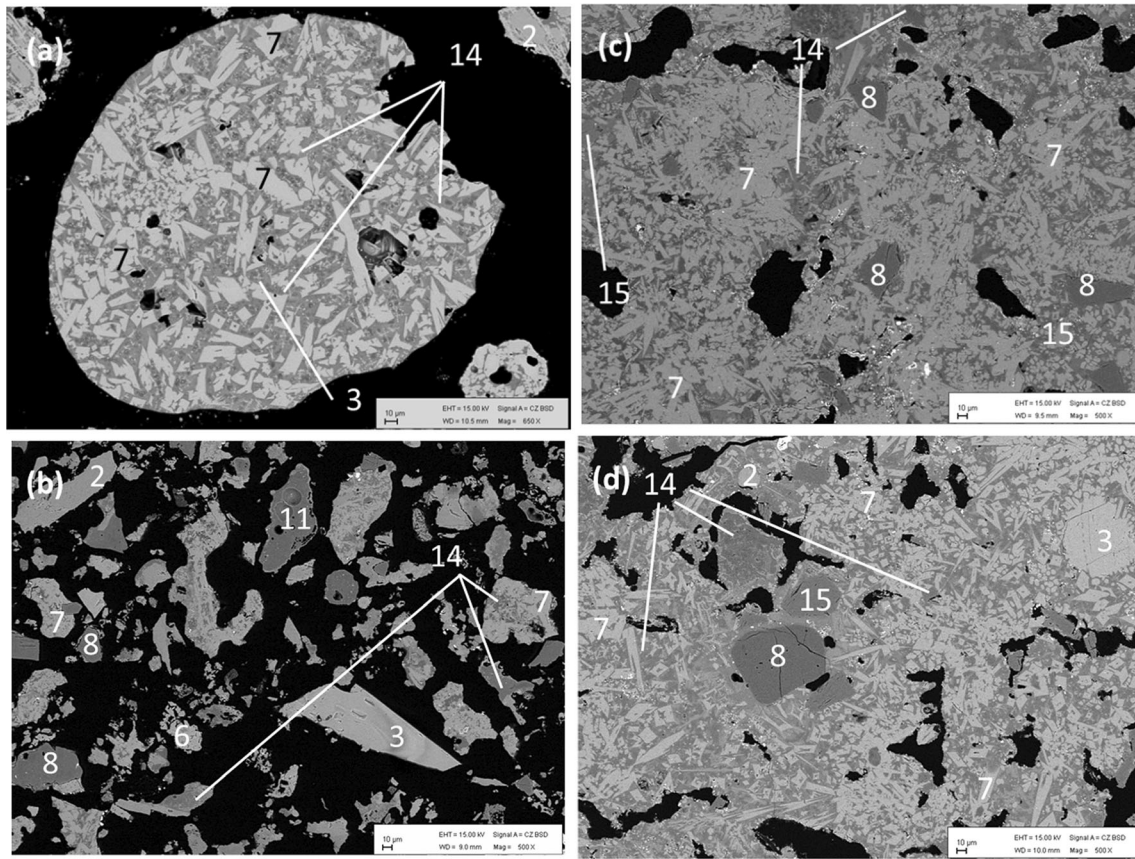
Fig. 4—Backscattered electron image of (*a*) MP 0, (*b*) MP 3, (*c*) MP 4, and (*d*) MP 6 after temperature treatment at 1100 °C for 10 minutes. (2) wollastonite, (3) fluorite, (7) cuspidine, (8) SiC, (11) slag, (14) liquid phase, and (15) diopside.

sintering tendency and marginal raw material residuals besides the liquid phase and cuspidine. Adding Si_3N_4 also results in a delay of the solid–solid reactions. Therefore, raw material particles and only small amounts of cuspidine were found.

After heat treatment at 1100 °C, most samples show a similar appearance: liquid phase and cuspidine crystals are formed [Figures 4(a, c, d)], and residuals of large raw material particles may still be found. However, in the case of MP 3, a partly liquid phase, which is not coherent, and cuspidine are present. A considerable quantity of raw material particles showing only a marginal reaction boundary at the particle surface, which indicates the beginning of new phase formation, is still present. In all specimens where SiC was added as a melt-controlling additive, SiC was found in the solid state in contact with the already-formed liquid phase, and these particles accumulate sometimes. The oxidation of the melt-controlling additive renders pores within the liquid phase. This can be observed particularly when silicon nitride is used. Furthermore, comparing the specimens at this temperature reveals that in the case of the granulated mold powder, each granule melts independently without forming a coherent liquid phase [Figures 4a, c, d)].

At 1200 °C, a liquid phase is formed in all cases. Although cuspidine crystals were observed in all samples, they were present during annealing at 1200 °C only in MP 0, MP 3, and partly in MP 5 because of their crystal shapes. In contrast, cuspidine revealed a stocky crystal shape during annealing [Figures 5(a and b): 7st.], and the dendritic crystals were formed when precipitating from the liquid during the quenching of the crucibles [Figures 5(b and c): 7dent.]. Additionally, for these three mold powders, residuals of SiC were found within the liquid phase. When the antioxidants were added, the residual particle size of MP 3 was reduced to approximately half of its original size. These results confirm the previously suggested assumption, based on the analysis of stepwise annealed samples at lower temperatures, that the addition of antioxidants Al and, particularly Si, diminishes the beneficial properties of SiC.

Mineralogical investigations of the as-received annealed mold powder revealed the unusual melting behavior of the granules, even at 1200 °C. Although all granules are at least partly in the liquid state, no coherent liquid phase is formed, and the granules remain separated. Some granules still showed cuspidine crystals, whereas others were completely liquified. Area scans of the granules using energy-dispersive X-ray spectroscopy

Fig. 5—Backscattered electron image of (*a*) MP 0, (*b*) MP 3, and (*c*) MP 5 after temperature treatment at 1200 °C for 10 minutes. (3) fluorite (7) cuspidine: stocky (st.) and dendritic (dent.), (8) SiC, and (14) liquid phase.

to quantify the chemical compositions of each granule revealed differences in their chemical compositions. Granules containing only the liquid phase showed slightly higher Na_2O and F contents than those containing the liquid phase and cuspidine; this results in the decrease in their melting temperature.

IV. CONCLUSION

The effect of various liquefaction-controlling additives on the melting behavior of the samples was investigated in comparison with a carbon-containing, as-received mold powder using thermodynamic calculations and mineralogical analysis of the stepwise annealed specimens. Both methods showed that SiC is a suitable replacement for carbon as the melting-controlling additive. At temperatures below 1100 °C, the formation of new phases *via* solid–solid diffusion is inhibited, and SiC remains in the solid state. Therefore, the necessary SiO_2 content to form a liquid phase is unavailable at lower temperatures. As the temperature increased and SiC oxidized, the availability of SiO_2 increased, which affected the stability of the new solid phases. Consequently, phases with lower silica contents were formed as long as SiC remained unoxidized. Moreover, the temperature of the first liquid phase and amount of liquid phase were affected. Although SiC-containing samples showed a lower solidus temperature compared with the mold powder as delivered (MP 0), their liquid phase amount after annealing at temperatures $\geq$ 1000 °C was still lower, which was consistent with the results of thermochemical calculations. Further addition of antioxidants, such as Al and Si, reduced the positive impact of SiC. Oxidation formed Al_2O_3 and SiO_2 which enhanced the reaction between raw material components owing to the increased liquid phase at approximately 900 °C. Si_3N_4 was another suitable carbon replacement for controlling the melting behavior of mold powders. The reactions between raw material particles were reduced significantly at temperatures below 1100 °C; above this temperature, the appearances of MP 0 and MP 8 were comparable. Comparing the images of mixtures with those of the granulated mold powder showed that the reaction velocity between the raw material particles was reduced at temperatures below 1000 °C. This was attributed to the production process of the granules, wherein a slurry of the raw materials was produced, leading to the dissolution of Na_2CO_3. Consequently, Na_2O delocalized and distributed over the whole volume[26] facilitating the formation of new phases with increasing temperature. Additionally, the contact between the raw material particles within one granule was closer than the particle contacts in loose powder mixtures, further influencing the reaction rate. The independent liquefaction of the granules without forming a coherent liquid phase even at 1200 °C was attributed to the production process of granulated mold powders. According to Reference 26 during spray drying, Na_2O diffused to the granule surface, leading to an increase in the Na_2O content. Consequently, during the high-temperature steps, each granule started to sinter from the outside, enclosing the solid components inside the hollow granule. Therefore, a liquid spherical boundary was present at each granule surface from the beginning of liquefaction. With the increasing liquid amount, each individual nearly spherical liquid drop approached its minimum surface energy. The formation of a coherent liquid containing all the granules of a specimen, especially by the consumption of
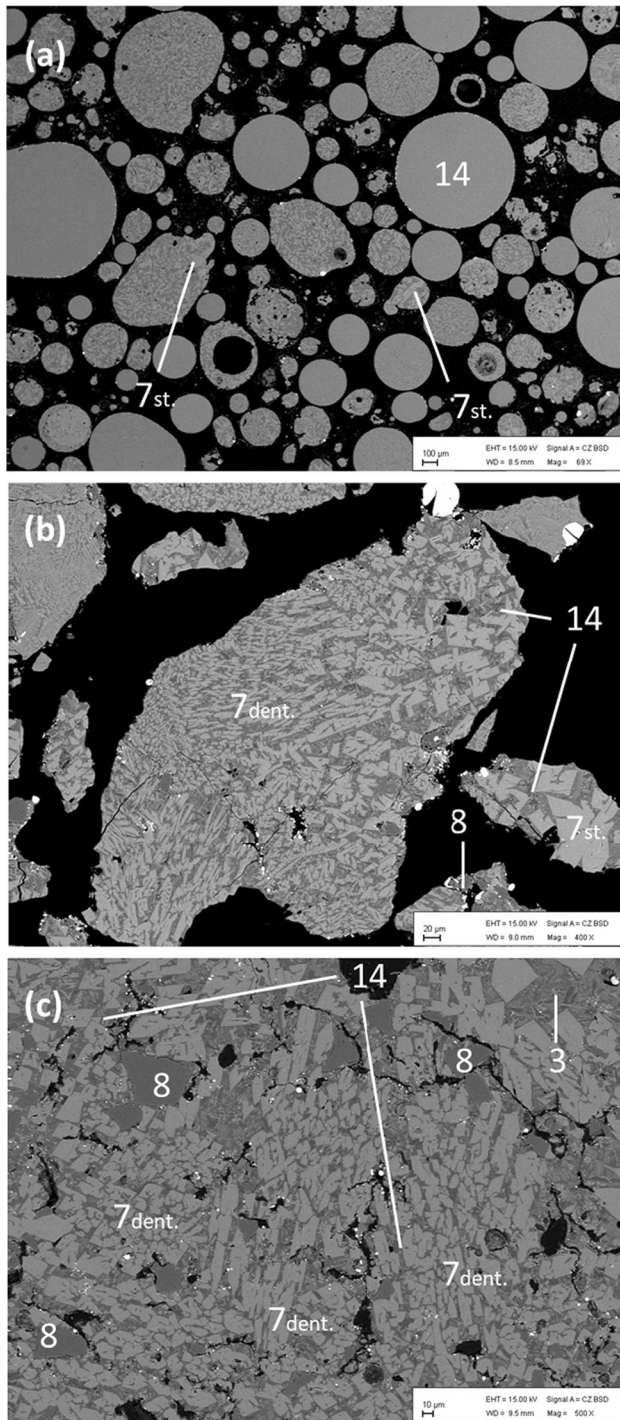
relatively small granules, further minimizes the total surface energy. While this process may have occurred partly in Figure 5(a), it remained incomplete owing to a lack of contact and time. This process may be facilitated during service associated with the lower viscosity at higher temperatures and contact with the slag pools.

Based on this study, it can be concluded that the amount of both SiC and Si_3N_4 can be further reduced to result in a melting behavior close to that of the standard mold powder. Therefore, depending on the production process of SiC and Si_3N_4, they may reduce the overall carbon content in the mold powder and CO_2 emission during casting.

CONFLICT OF INTEREST

The author declares that she has no conflict of interest.

REFERENCES

1. K.C. Mills, A.B. Fox, R.P. Thackray, and Z. Li: in *Proc. of VII Int. Conf. on Molten Slags, Fluxes & Salts*. M. Sanchez, ed., The South African Institute of Mining and Metallurgy, Johannesburg, 2004, pp. 713–22.
2. K. C. Mills: *NPLRep. DMM(A)*, ECSC Contract No. 7210.22/451, Report EUR 13177 EN, Teddington, U.K., 1990.
3. M. Kawamoto, K. Nakajima, T. Kanazawa, and K. Nakai: *ISIJ Int.*, 1994, vol. 34, pp. 593–98.
4. N. Kölbl, I. Marschall, and H. Harmuth: in *Proc. of VIII Int. Conf. on Molten Slags, Fluxes & Salts*. M. Sanchez, ed., Santiago, Chile, 2009, pp. 1031–40.
5. J. A. Kromhout: *Mould powders for high speed continuous casting of steel*, PhD Thesis, Technical University Delft, Delft, 2013. http://resolver.tudelft.nl/uuid:4b52997d-9fc9-41b3-a4e8-70ffab1b3fdf.
6. M. Supradist, A.W. Cramb, and K. Schwerdtfeger: *ISIJ Int.*, 2004, vol. 44, pp. 817–26.
7. W. Yan, Y.D. Yang, W.Q. Chen, M. Barati, and A. McLean: *Can. Metall. Q.*, 2015, vol. 54, pp. 467–76.
8. Z.M. Yi, J.L. Song, and Q.C. Peng: *Adv. Mater. Res.*, 2013, vol. 739, pp. 214–17.
9. S. Terada, S. Kaneko, T. Ishikawa, and Y. Yoshida: *Iron Steelmak.*, 1991, vol. 18, pp. 41–44.
10. F. Han, G. Wen, P. Tang, and F. Chen: *Metall. Mater. Trans. B*, 2023. Unpublished research.
11. H. Nakato, S. Takeuchi, T. Fujii, T. Nozaki, and M. Washio: in *75th Steelmak. Conf. Proc.*, Washington DC, USA, 1991, pp. 639–46.
12. H. Takeuchi, H. Mori, T. Nishida, T. Yanai, and K. Mukunashi: *Tetsu-to-Hagané*, 1978, vol. 64, pp. 1548–57.
13. H. Takeuchi, T. Nishida, T. Ohno, N. Kataoko, and Y. Hikara: Deutsches Patent (26 26 354), 1976, München, Deutschland: Deutsches Patentamt.
14. B. Debiesme, J. P. Radot, D. Coulombet, C. Lefebvre, J. N. Pontoire, Y. Roux, and C. Damerval: United States Patent (5,876,482), 1996, Washington D.C.: U.S. Patent and Trademark Office.
15. B. Debiesme, J. P. Radot, D. Coulombet, C. Lefebvre, J. N. Pontoire, Y. Roux, and C. Damerval: United States Patent (6,328,781), 1998, Washington D.C.: U.S. Patent and Trademark Office.
16. C. Lefebvre, J.P. Radot, J.N. Pontoir, and Y. Roux: *La Revue de Métallurgie-CIT*, 1996, pp. 489–96.
17. L. Sun, C. Liu, J. Fang, J. Zhang, and C. Lu: *J. Eur. Ceram. Soc.*, 2019, vol. 39, pp. 1532–39.
18. J.J. Macho, G. Hecko, B. Golinmowski, and M. Frazee: in *Preprints 33rd McMaster Symp. on Iron and Steelmaking*. McMaster Univ., Hamilton, 2005, pp. 131–46.
19. J. Safarian and M. Tangstad: *Metall. Mater. Trans. B*, 2009, vol. 40B, pp. 920–28.
20. J. Park, J. Jeon, K. Lee, J.H. Park, and Y. Chung: *Metall. Mater. Trans. B*, 2016, vol. 47B, pp. 1832–38.
21. O. Maillart, V. Chaumat, and F. Hodaj: *J. Mater. Sci.*, 2010, vol. 45, pp. 2126–32.
22. L. Ning and Ch. Jinghao: *J. Shaoguan Univ.*, 1998, vol. 19, pp. 112–20.
23. Taikabutsu Gijutsu Kyōkai (Japan): *Refractories Handbook*, The Technical Association of Refractories, Japan, 1998.
24. T. Wang and A. Yamaguchi: *J. Am. Ceram. Soc.*, 2001, vol. 84, pp. 577–82.
25. N.K. Ghosh, K.P. Jagannathan, and D.N. Ghosh: *Interceram*, 2001, vol. 50, pp. 196–202.
26. F. Han, L. Yu, G. Wen, X. Wang, F. Zhang, J. Jia, and S. Gu: *J. Mater. Res. Technol.*, 2022, vol. 20, pp. 448–58.

Publisher's Note Springer Nature remains neutral with regard to jurisdictional claims in published maps and institutional affiliations.